Research in Pharmaceutical Sciences, October 2019; 14(5): 378-390
Received: October 2018
Accepted: April 2019

School of Pharmacy & Pharmaceutical Sciences
Isfahan University of Medical Sciences

Original Article

Understanding the effect of lipid formulation loading and ethanol as a diluent on solidification of pitavastatin super-saturable SNEDDS using factorial design approach

Ilham Kuncahyo[1,2], Syaiful Choiri[3,*], Achmad Fudholi[4], Abdul Rohman[5,*], and Ronny Martien[4]

[1]Faculty of Pharmacy, Gadjah Mada University, Sekip Utara, Yogyakarta, Indonesia.
[2]Department of Pharmaceutical Science, Setia Budi University, Surakarta, Indonesia.
[3]Drug Delivery and Pharmaceutical Technology, Pharmaceutics Research Group, Department of Pharmacy, Universitas Sebelas Maret, Ir. Sutami 36A, Surakarta, Indonesia.
[4]Department of Pharmaceutics, Gadjah Mada University, Sekip Utara, Yogyakarta, Indonesia.
[5]Department of Pharmaceutical Chemistry, Gadjah Mada University, Sekip Utara, Yogyakarta, Indonesia.

Abstract

Solidification of a preconcentrate lipid formulation namely self-nano emulsifying drug delivery system (SNEDDS) is required to achieve feasibility, flexibility, and a new concept of "dry nano-emulsion". The purpose of this study was to assess the effect of SNEDDS loading and ethanol as a diluent on the solidification of pitavastatin supersaturable SNEDDS (S-SNEDDS). A 2^2 full factorial design approach with a center point addition as a curvature was implemented to determine the effect of S-SNEDDS loading and ethanol on the physical characteristics, namely flowability, compactibility, and drug release behavior. Vibrational spectra, thermal behavior, and morphology of solid S-SNEDDS formulation were also evaluated. The results indicated that there was no interaction between S-SNEDDS and carrier, based on vibrational spectra. However, thermal behaviors (enthalpy and weight loss) were depending on SNEDDS loading. Thereafter, the ethanol as a diluent of preconcentrated formulation had no effect on the morphology of carrier structure. However, the S-SNEDDS loading altered the structure of carrier owing to either solubilization or abrasion processes. The statistical model suggested that ethanol as diluent reduced the flowability, compactibility, and drug releases. Meanwhile, the liquid SNEDDS loading affected the reducing of flowability and compactibility. Finally, solidification without diluent and 20% lipid formulation load was recommended. In addition, it was very useful because of ease on handling, flexibility for further formulation, and desired characteristics of final solid dosage form.

Keywords: Pitavastatin; Solidification; Solid SNEDDS; Supersaturable.

INTRODUCTION

Lipid formulation gains a great attention for improving bioavailability of the poorly water-soluble drug. Nano-emulsion formed by low energy *i.e.* self-nano formation during dilution with medium is attractive manner because of its cost-friendly and simple technology method (1,2). Supersaturable self-nano emulsifying drug delivery system (S-SNEDDS) is a preconcentrate of lipid formulation comprising of oil, surfactant, and co-surfactant in which the drug is incorporated into them until the saturated condition is achieved at a predetermined condition. This formulation formed nanodroplet by dilution with medium (3,4). The S-SNEDDS formulation has several advantages which include the enhancement of drug effectiveness owing to a high drug loading, avoiding the high amount of surfactant (5), and achieving flexibility to adjust the dose for medium to high potency drugs (6,7).

Access this article online

Website: http://rps.mui.ac.ir

DOI: 10.4103/1735-5362.268198

*Corresponding authors:
S.Choiri, Tel: +62-271669376, Fax: +62-271663375
Email: syaiful.apt@gmail.com
A. Rohman, Tel: +62-274543120, Fax: +62-274543120
Email: abdul_kimfar@ugm.ac.id

However, liquid lipid formulation is not suitable for further formulation development owing to the requirement of sophisticated instrument and formulation *e.g.* soft capsules and issues related to the physical stability (5). Furthermore, the solidification of lipid formulation is required to enhance its flexibility and feasibility for the further development processes *e.g.* tablet, granule/powder filled to capsule formulation, and a new concept of dry nanoemulsion (8,9). In addition, the solidification of liquid SNEDDS formulation is attractive and applicable for pharmaceutical industries (10).

Solidification means alteration of the liquid phase of SNEDDS to solid-state phase using absorption and adsorption phenomena on a carrier. The carrier involves water-soluble/insoluble characteristics (11,12). Currently, in order to achieve a new concept of "dry nano-emulsion", solidification using a water-soluble carrier which does not affect nanodroplet formation of nanoemulsion during solubilization is an interesting manner (13). Mannitol, a freely water-soluble carrier, was modified physically to obtain a spherical inner porous material under a spray-drying technique. This modification enhanced the surface area, hence it could increase the ability of liquid S-SNEDDS formulation to be incorporated into the inner core of carrier (14,15). However, the solidification of liquid S-SNEDDS is also affected by several factors, namely SNEDDS loading, the viscosity of SNEDDS, pore of material, absorption or adsorption mechanism, characteristics of the native solid carrier, and the interaction between them (4,9,12,16). SNEDDS loading affects the physico-mechanical properties of solid SNEDDS formulation *e.g.* flowability and compactibility. The viscosity of lipid formulation governs flexibility of the liquid phase to be incorporated and impregnated into the carrier through the porous system (7,9). According to the characteristics of mannitol as a water-soluble carrier, the incorporation of SNEDDS into the carrier involves the absorption mechanism, in which the SNEDDS formulation passes through the porous and distribute in the surface of carrier (4). Hence, the greater surface area, the higher load of SNEDDS formulation is (14). Reducing the thickening of the SNEDDS formulation can be used to facilitate and make it easy in the incorporation into porous carrier, and acting as diluent (co-surfactant).

In order to assess the crucial factor on solidification *i.e.* SNEDDS loading and diluent to reduce the viscosity, design of experiment based on 2^2 full factorial design applied with the addition of center point as a curvature. Several studies have reported that it enhanced the predictive power of the model (17,18). To the best of our knowledge, there were no reported data about the effect of the prior process on the incorporation of lipid formulation into a carrier. Therefore, the purpose of this study was to assess the effect of S-SNEDDS loading and ethanol as thickening reduction of SNEDDS on solidification process of SNEDDS formulation. Thereafter, the design of experiment could suggest the controlled space under statistical investigation and simultaneous assessment of those factors.

MATERIAL AND METHODS

Materials

Capryol® and Transcutol® P were obtained from Gattefose (Saint Priest, France). Tween® 80 was purchased from Sigma Aldrich (St. Louis, MO, USA), and ethanol and ammonium carbonate were obtained from Merck (Darmstadt, Germany). Ca-pitavastatin (PVT) was purchased from Thanen Chemical Co. Ltd (Xinbei District, China). Mannitol was obtained from Roquette (Lestrem, France).

Preparation and characterization of super-saturable self-nano emulsifying drug delivery system

Preparation of S-SNEDDS was carried out according to the previous methods with slight modification (7). According to our preliminary study, the optimized formula comprising of 23.4% Capryol®, 35.6% Tween® 80, and 40.0% Transcutol® P was prepared separately depending on their composition for each run. Those components were mixed together using a Branson U-2510 ultrasonicator (Danbury, CT, USA) and stirred at 500 rpm using an IKA

C-MAG HS7 magnetic stirrer (Staufen, Germany) for 5 min. An excess amount of PVT was added until a saturated condition was achieved (mixing for approximately 72 h at ambient temperature, 26 ± 1°C). The mixture was centrifuged at 15000 *g* for 45 min using a MicroCL Thermo centrifuge (Waltham, MA, USA), and the supernatant was collected as the S-SNEDDS formulation. The amount of PVT loaded in the S-SNEDDS formulation was determined using a Hitachi U-2900 UV-Vis spectrophotometer (Tokyo, Japan) after dilution with methanol at a wavelength of 244 nm under validated analytical method (R^2 = 0.998; recovery = 102.82%; and precision = 1.70%).

In order to characterize SNEDDS, one part of S-SNEDDS was diluted with 100 part of water (37 °C) under gently agitation (50 rpm) for 5 min at ambient temperature. The droplet size and zeta potential were measured using a Horiba SZ-100 particle size analyzer (Kyoto, Japan). The measurement was performed using a dynamic light scattering technique at a wavelength of 632 nm, angle 173° and a refractive index of 1.333, and sample absorbance was adjusted according to the absorbance of the sample. Gate time was adjusted in a range of 2.56 to 10.24 μs to achieve appropriate condition for measurement. Zeta potential was measured using carbon cuvette at 25°C.

Preparation and characterization of water-soluble porous carrier

The water-soluble porous material was prepared by a spray drying method according to Peng's method with a minor modification (14). Briefly, mannitol 92.5% and ammonium carbonate 7.5% were dissolved in water at a total solid concentration of 15% (w/v). The solution was dried using a Buchi mini spray dryer B-290 (Flawil, Switzerland). The spray dryer was conditioned at the inlet and outlet temperature of 120 and 50°C, respectively, aspirator of 90%, and pump level of 25%, and pressure of -50 mbar. The solidified mannitol was collected and stored in the desiccator until further characterization and formulation.

Characterizations of porous mannitol *e.g.* specific surface area, pore size, and pore volume were measured using a Quadrasorb evo surface area analyzer (Boynton Beach, FL, USA). The sample was degassed under vacuum for 12 h prior to measurement. These results were calculated using Brunauer-Emmet-Teller analysis.

Design of experiment for solidification of self-nano emulsifying drug delivery system

A 2^2 full factorial design with the addition of a center point as a curvature was applied to assess the effect of lipid formulation (S-SNEDDS) loading and ethanol as a diluent on the solidification process. Five runs comprising of four design points as model design and one point in the middle of the design as a curvature was constructed. Two factors namely SNEDDS loading and amount of ethanol (presented in ethanol to S-SNEDDS ratio) were used at two levels, as presented in Table 1. These factors were determined on the flowability *i.e.* angle of repose, compactibility, drug load, and the drug release. Each point of the design was carried out in triplicates.

Table 1. Experimental design of 22 full factorial design with curvature for solidification of supersaturable self-nano emulsifying drug delivery system (S-SSNEDDS) formulation.

Types	Runs	SNEDDS (%)	Ethanol to SNEDDS ratio
Design points	R1	10	0
	R2	20	0
	R3	10	1
	R4	20	1
Additional point	Curvature	15	0.5

Solidification of super-saturable self-nano emulsifying drug delivery system

Incorporation of SNEDDS into solid carrier adopted from a previous reported study with a minor modification (19). Briefly, 10 g of the water-soluble porous carrier was weighed accurately. Furthermore, an amount of SNEDDS and ethanol according to the composition as aforementioned in the Table 1 was withdrawn and mixed together until a homogenous mixture was achieved. The water-soluble porous carrier was added carefully to the mixture using a spatula. The homogeneity of solid-SNEDDS was ensured until the relative standard deviation of PVT content less than 5% was achieved. The solid SNEDDS formulation was stored in the desiccator until further characterizations were evaluated.

Characterization solid super-saturable self-nano emulsifying drug delivery system

The solid S-SNEDDS characterization was performed using infrared spectrophotometer, thermal analyses, and morphological/surface imaging. Vibrational spectra of the PVT and solid S-SNEDDSs were analyzed using Thermo Nicolet i50 Fourier transform infrared (FTIR) spectrophotometer (Waltham, MA, USA) equipped with attenuated total reflectance (ATR) with ZnSe crystal as sampling handling technique and deuterated triglycine sulfate detector. The sample was placed on ATR crystal and scanned from 650-4000 cm^{-1} with a resolution of 2 cm^{-1} and 32 scanning.

Thermal behavior of the PVT and solid S-SNEDDS was characterized using Shimadzu DSC-60 differential scanning calorimeter (DSC) and Shimadzu DTG-60 thermal gravimetric analyzer (Kyoto, Japan). An approximate of 5 mg sample was placed into an Al_2O_3 (aluminum hermetic) pan and heated from 30 to 300 °C at a rate of 10 °C/min under a 30 mL/min nitrogen atmosphere. An empty pan was used as a reference. The temperature and enthalpy were calibrated using a standard indium.

Morphology characterization of PVT and solid S-SNEDDS was performed using a JEOL JSM-6510LA scanning electron microscopy (SEM) (Tokyo, Japan). The sample was coated with a platinum for 130 s using a JEOL JEC-3000PC auto fine coater (Tokyo, Japan). Samples were observed at an accelerating voltage of 5 kV using several magnifications until the desired photograph was achieved.

Physical properties and drug load of solid super-saturable self-nano emulsifying drug delivery system characterization

The physical properties of solid S-SNEDDS were characterized by flowability and compactibility which are presented by angle of repose and tensile strength, respectively. The drug load was also characterized.

Angle of repose was performed by solid S-SNEDDS through an orifice. A 10 g of solid S-SNEDDS was passed through an orifice (opening diameter 125 mm and orifice diameter 12 mm). The powder was allowed to pass through the orifice, and the diameter (d) and height (h) of the powder pile were measured manually using a Mitutoyo caliper (Tokyo, Japan) with the accuracy of 0.01 mm. The angle of repose could be calculated using equation 1 (20).

$$\tan(\text{Angle of repose}) = 2h/d \qquad (1)$$

The compactibility was measured according to the tensile strength of the tablet. A 200 mg of solid S-SNEDDS powder was weighed and filled manually in the 7 mm die equipped with a flat-face punch. The powder was compressed into a tablet at a similar compression force. The tablet crushing strength (F) was measured using a Stokes Monsanto hardness tester (Warrington, PA, USA). Prior to the measurement of the tablet crushing strength, the tablet diameter (d) and height (h) were measured using a caliper. The tensile strength was calculated using equation 2 (21).

$$\text{Tensile strength} = 2F/dh \qquad (2)$$

Drug load was measured according to the amount of PVT in 1 g of solid S-SNEDDS formulation. One hundred mg of solid S-SNEDDS formulation was weighed accurately and dissolved in methanol followed by a sonication for 15 min. Thereafter, it was filtered using a 0.45 μm membrane filter

and diluted until an appropriate response was achieved. The sample was analyzed spectrophotometrically under a validated analytical method (wavelength 244 nm; $R^2 = 0.998$; recovery = 102.82%; and precision = 1.70%).

Drug release from solid super-saturable self-nano emulsifying drug delivery system

The drug release was characterized by *in vitro* drug release study according to the Dash *et al.* (19) and Zhao *et al.* (22) methods with a minor modification. The solid SNEDDS formulation equivalent to 2 mg of Ca-PVT was weighed accurately for each run. Furthermore, it was filled into a hard gelatin capsule. The characterization of drug release was carried out using an Erweka DT-820 dissolution tester (Heusenstamm, Germany) equipped with a USP model type I (basket). Nine hundred mL simulated gastric fluid was used as a medium and the temperature was kept constant at 37 ± 0.5 °C with agitation of 100 rpm. The sample was withdrawn at predetermined times *i.e.* 1, 3, 5, 7, 10, 20, and 30 min and analyzed using ultraviolet spectrophotometer at 248 nm under a validated analytical method (R^2 = 0.999; recovery = 99.27%; and precision = 1.08%). In order to compare the dissolution profile, dissolution efficiency was implemented and calculated using equation 3 according to the percentage of drug released (y) in determined time (t) and total time to be calculated (T) (23).

$$\text{Dissolution efficiency} = \frac{\int_0^t y\delta t}{100\,T} \times 100\% \qquad (3)$$

Optimization and statistical analysis

The main effect and two-factor interaction models were generated for all the response variables using a multiple linear regression analysis (MLRA). Each model was evaluated based on several statistical parameters, including the coefficient of determination (R^2), adjusted coefficient of determination (Adj. R^2), predicted coefficient of determination (Pred. R^2), adequate precision, and predicted residual error sum square.

A significant effect on response was determined by F test or *P*-value of analysis of variance (ANOVA), calculated using Design-Expert software, with a confidence level of 95% (P = 0.05). A contour plot was constructed based on the model equation of each response. Superimposed contour plot was used to determine the optimized region based on product performance by combining the contour plot of each model (24).

RESULTS

Self-nano emulsifying drug delivery system characterization

PVT was successfully loaded into S-SNEDDS formulation, corresponding to 74.01 ± 5.00 mg PVT in each gram of S-SNEDDS formulation. Nano-emulsion formed by dilution had droplet size and zeta potential of 73.10 ± 7.35 nm and -34.70 ± 2.64 mV, respectively.

Porous mannitol characterization

The yield of porous carrier was 82.45%. According to Brunauer-Emmet-Teller analysis results (Table 2), the total surface area of porous mannitol (6.831 ± 0.049 m^2/g) was higher than that of unprocessed mannitol (5.926 ± 0.072 m^2/g) ($P < 0.05$). Meanwhile, pore size and pore volume of porous mannitol (4.138 ± 0.008 nm and 9.178 ± 0.118 mL/g, respectively) were higher than those of unprocessed mannitol (3.650 ± 0.007 nm and 7.268 ± 0.123 mL/g) ($P < 0.05$). These results revealed that the addition of pore-promoting agent generated the porous mannitol.

Table 2. Characteristics of mannitol and modified mannitol according to the Brunauer-Emmet-Teller analysis.

Parameters	Mannitol (± SD)	Mesoporous mannitol (± SD)
True density (g/mL)	1.168	1.198
Total surface area (m^2/g)	5.926 ± 0.072	6.831 ± 0.049*
Pore size (nm)	3.650 ± 0.007	4.138 ± 0.008*
Pore volume (mL/g) × 10^{-3}	7.268 ± 0.123	9.178 ± 0.118*

* Considered statistically significant between mannitol and mesoporous mannitol groups, $P < 0.05$.

Attenuated total reflectance-FTIR characterization

The vibrational spectra of PVT and solid S-SNEDDS are presented in Fig. 1. The FTIR spectrum of mannitol porous carrier (Fig. 1a) was assigned by specific vibrational peaks, namely OH hydrogen bonding and free OH stretching vibrations which appeared at the wavenumbers of 3286 and 3463 cm^{-1}, respectively. The peaks at 1022 and 1084 cm^{-1} were due to C-O stretching vibrations. The alkyl vibration of mannitol porous was assigned around 1450-1300 cm^{-1}.

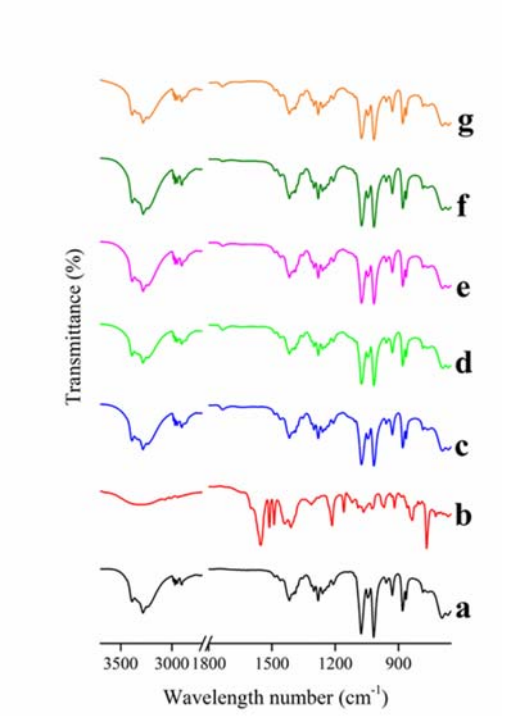

Fig. 1. ATR-FTIR spectra of (a) mannitol meso-porous carrier, (b) pitavastatin, (c) run 1 (10% SNEDDS load without ethanol), (d) run 2 (20% SNEDDS load without ethanol), (e) run 3 (10% SNEDDS load with ethanol), (f) run 4 (20% SNEDDS load with ethanol), and (g) run 5 (center of the design). ATR-FTIR, Attenuated total reflectance Fourier transform infrared; SNEDDS, self-nano emulsifying drug delivery system

In addition, the vibrational peak of PVT (Fig. 1b) was assigned by carbonyl (C=O) stretching vibration at 1645 cm^{-1}, O-H carboxylic at 3340 cm^{-1}, halogen (C-F) vibration at 748 cm^{-1}, and C-O vibration at 1206 cm^{-1}. Furthermore, the vibrational peak of various formulations (Fig. 1c-1f) according to the level of S-SNEDDS loading and ethanol had a similar pattern with a negligible peak shifting. The similar vibrational peak patterns of all formulations were caused by no interaction between SNEDDS and porous carrier. However, the carrier peak vibration was dominant compared to PVT peaks.

Differential scanning calorimetry and thermogravimetry characterization

The thermal behaviors of PVT and solid S-SNEDDS were evaluated using DSC-TGA as shown in Fig. 2. PVT (Fig. 2a) showed a broad endothermic peak around 70-120 °C owing to the dehydration of water adsorption and hydrate in the crystal lattice structure which was confirmed by 11.2% weight loss.

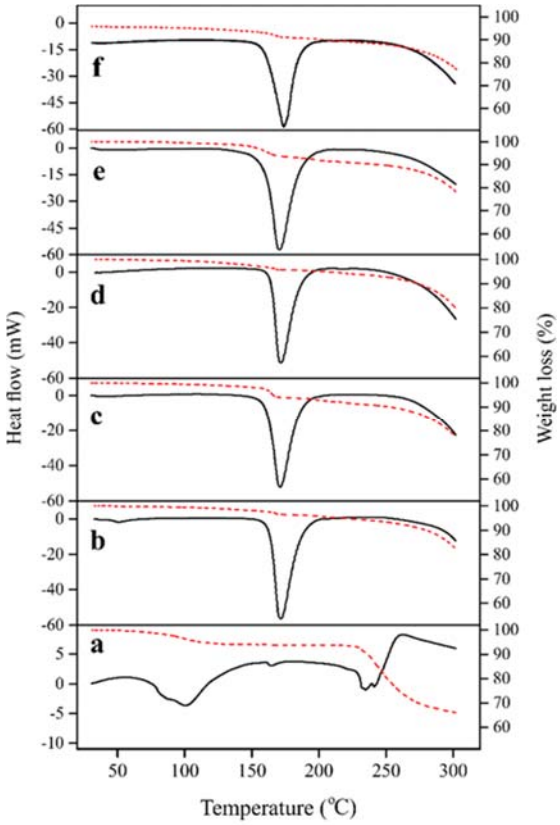

Fig. 2. DSC-TGA thermograms of (a) pitavastatin, (b) run 1 (10% SNEDDS load without ethanol), (c) run 2 (20% SNEDDS load without ethanol), (d) run 3 (10% SNEDDS load with ethanol), (e) run 4 (20% SNEDDS load with ethanol), and (f) run 5 (center of the design). DSC-TGA, differential scanning calorimeter-thermogravimetry; SNEDDS, self-nano emulsifying drug delivery system.

An endothermic peak was observed at 225.3 °C according to PVT melting point and

followed by its decomposition which was confirmed by the TGA thermogram (35% weight loss up to 300 °C). DSC thermogram of all solid S-SNEDDS formulations exhibited a sharp endothermic peak at 170-171 °C according to the melting point of mannitol. All formulations (Fig. 2b-2f) showed similar pattern of DSC thermograms, however, it could be differentiated from the enthalpy values. The higher SNEDDS load, the lower enthalpy was. The TGA thermogram showed a similar pattern as indicated by the presence of weight loss around 160-170 °C according to the decomposition of SNEDSS components. It was different from the amount of weight loss, the higher the SNEDDS load, the greater the weight loss. In addition, there was no crystallization of PVT during the solidification owing to the disappearance of endothermic peak of PVT. The enthalpy of run 2 was higher than of run 4 as same as the weight loss of run 2 was lower than that of run 4. Run 5 lied in the mean of enthalpy of run 4 and run 2. These results suggested that the presence of ethanol could not be eliminated during the solidification.

Morphological characterization

In order to understand the effect of these factors on the morphological characteristic of solid S-SNEDDS and the probability of crystallization, SEM photographs of PVT, mannitol porous carrier, and solid S-SNEDDS formulations are presented in Fig. 3. The carrier morphology showed almost spherical form with a crystalline structure of mannitol. Moreover, the carrier had a hollow space in the core of the carrier. Thus, the carrier was called micro-spherical porous carrier. Morphology of all formulations is presented in Fig. 3. Generally, all formulations had different surface morphological characteristics compared to the native carrier. All formulations had a rough surface owing to a partial solubilization of carrier using the SNEDDS characteristics in which a part of mannitol was soluble in SNEDDS formulation. On the other hand, ethanol did not solubilize the mannitol.

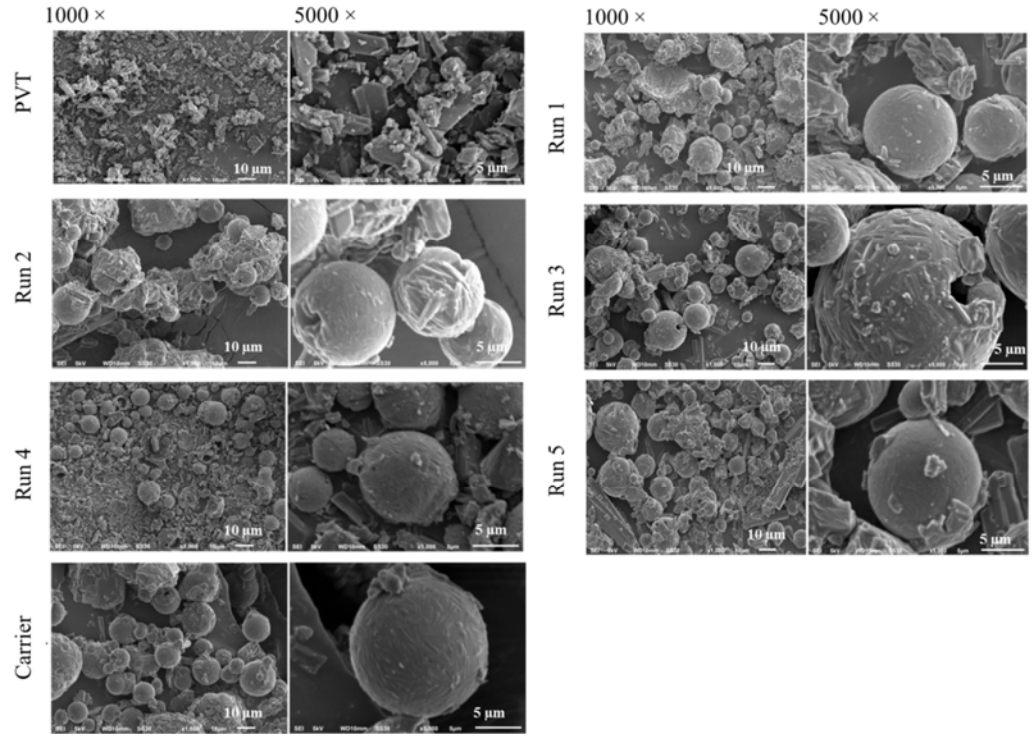

Fig. 3. SEM photograph of pitavastatin, mannitol porous carrier, and solid S-SNEDDSs including run 1 (10% SNEDDS load without ethanol, run 2 (20% SNEDDS load without ethanol), run 3 (10% SNEDDS load with ethanol), run 4 (20% SNEDDS load with ethanol), and run 5 (center of the design). SEM, Scanning electron microscopy; PVT, pitavastatin; S-SNEDDS, supersaturable self-nano emulsifying drug delivery system.

Statistical parameters of design of experiment

In order to assess the effect of S-SNEDDS load and ethanol as the diluent on the flowability and drug released behavior, the 2^2 factorial design with an addition of one point as a curvature was implemented. All responses had significant models ($P < 0.05$) and the curvatures were not significant ($P > 0.05$). The best-fitting model was described by the goodness of fit, i.e. coefficient of determination (R^2) more than 0.7 meaning that the percentage of factors affected to the response was (> 70%) as well as the difference between adjusted R^2 and predicted R^2 was less than 0.2. The predicted R^2 obtained from the internal validation of the model using cross-validation with leave one out technique, and signal to noise ratio assigned as adequate precision more than 4 (24). All statistical parameters are resumed in Table 3. All models of all responses met these requirements. Thus, it could be applied for leading the effect of factor on responses.

Flowability and compactibility

According to MLRA approach of angle of repose (Table 3), S-SNEDDS loading (0.20) did not significantly affect angle of repose ($P > 0.05$), while the ethanol (1.32) had significant effect on increasing the angle of repose ($P < 0.05$). In addition, the interaction of both factors (0.20) had no significant effect on angle of repose ($P > 0.05$). Figure 4a depicted the contour plot of angle of repose. The highest angle of repose was obtained at the high level of ethanol, and the lowest angle of repose was obtained at solid S-SNEDDS without ethanol. The drug load of all formulations was only affected by S-SNEDDS loading owing to the contained drug in the S-SNEDDS formulation. The linear function was observed on an increase of the S-SNEDDS loading in which the highest drug load was obtained at the high level of SNEDDS loading and decreased as decreasing the S-SNEDDS loading level. The physico-mechanical characteristic of S-SNEDDS powder was measured using a tablet tensile strength. According to the MLRA approach of tensile strength (Table 3), SNEDDS loading (-7.06) had higher effect on reducing the tensile strength than ethanol (-3.29), and both factors were statistically significant ($P < 0.05$). Although, the interaction between both factors were not significant ($P > 0.05$). Contour plot of tensile strength is presented in Fig. 4b. The highest tensile strength was obtained at the lower level of both factors. On the other hand, the lowest tensile strength was observed at the highest level of both factors. A linear function was observed owing to the insignificant interaction of both factors.

Table 3. Statistical parameter of factorial design for solidification of super-saturable self-nano emulsifying drug delivery system formulation.

Parameters	AoR (degree)		Tensile strength (N/cm^2)		DL (mg/g)		Q_{3min} (%)		DE_{7min} (%)	
	Coef.	***P*-value**	**Coef.**	***P*-value**	**Coef × 10^{-2}**	***P*-value**	**Coef.**	***P*-value**	**Coef.**	***P*-value**
Intercept	37.88	-	19.67	-	69	-	65.75	-	65.97	-
A	0.20*	0.046	-7.06	< 0.0001	18	< 0.0001	6.66	0.0036	3.62	0.0122
B	1.32	0.001	-3.29	< 0.0001	-0.32*	0.4514	-7.96	0.0011	-2.22*	0.0910
AB	0.20*	0.459	0.16	0.7501*	0.008*	0.8350	-7.82	0.0013	-5.70	0.0007
Model		0.0040		< 0.0001		< 0.0001		0.0002		0.0012
Curvature		0.9875*		0.1099*		0.0672*		0.7903*		
R^2	0.7214		0.9624		0.9949		0.8444		0.7820	
Adjusted R^2	0.6378		0.9512		0.9934		0.7977		0.7166	
Predicted R^2	0.3732		0.9155		0.9886		0.6499		0.5096	
PRESS	19.08		63.87		0.0005		840.42		380.62	
Adeq. Prec	5.742		21.266		45.104		8.946		7.855	

A, Self-nano emulsifying drug delivery system loading (Level); B, ethanol (level); AoR, angle of repose; Coef, regression coefficient; DL, drug loading; Q_{3min}, amount of drug released during 3 min; DE_{7min}, dissolution efficiency during 7 min; R^2, coefficient of determination; PRESS, predicted residual error sum square; Adeq. Prec, adequate precision; *, statistically not significant difference ($P > 0.05$).

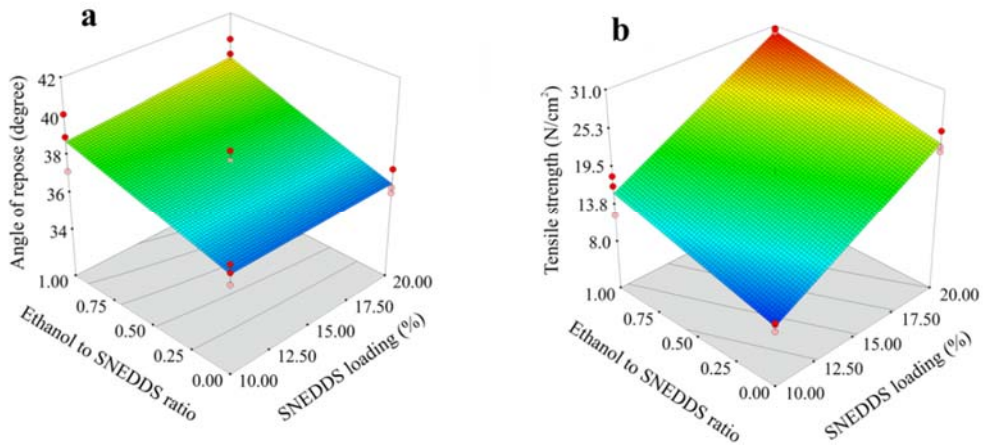

Fig. 4. Contour plot of (a) angle of repose and (b) tensile strength. SNEDDS, self-nano emulsifying drug delivery system

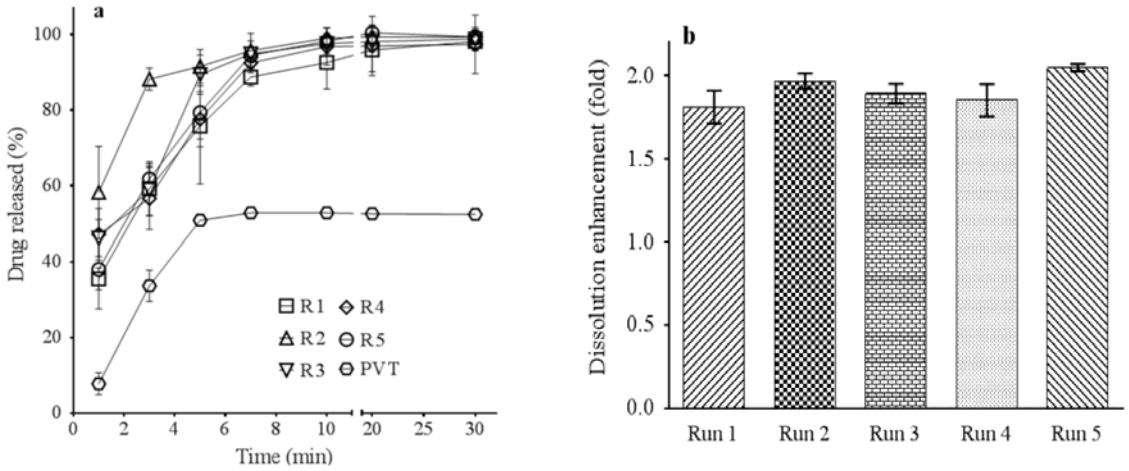

Fig. 5. (a) Drug release profiles of pitavastatin and solid S-SNEDDS formulation under different runs and (b) dissolution enhancement of solid S-SNEDDS. Calculated based on relative area under dissolution curve. PVT, pitavastatin; S-SNEDDS, supersaturable self-nano emulsifying drug delivery system.

Drug loading

The MLRA of drug loading (Table 3) reveled that only SNEDDS loading had significant effect on drug load (98.2% of factor contribution) ($P < 0.05$). The SNEDDS contained the drug which contributed to the drug load parameter. On the other side, the ethanol did not alter the drug load parameter (1.75% factor contribution). Interaction of both factors (0.04% interaction contribution) was not significant ($P > 0.05$). The drug load model was constructed to evaluate the effect of ethanol on solidification i.e. SNEDDS distribution during solidification. Thus, this factor was not attractive for further discussion owing to no interaction and significant effect of diluent.

Drug release characterization

In order to characterize the drug release behavior of solid SNEDDS, the dissolution study of all formulations was performed. The term of drug release means the formation of the nano-droplet during carrier solubilization or SNEDDS formulation release from carrier. The drug release profiles of all formulations and PVT are presented in Fig. 5a. All solid S-SNEDDS formulations had higher drug released compared to the PVT. The drug release profiles showed that different drug release profile observed in the initial time. In addition, the drug release profiles over 3 min did not differ from each run. All formulations had no significant effect on the enhancement of the drug release profile (Fig. 5b) in range of 1.8-2.1 folds ($P > 0.05$).

Thus, 50% of the PVT was released for 30 min. Meanwhile, all formulations released 100% for 7 min. This result suggested that the solid S-SNEDDS formulation enhanced the drug released significantly ($P < 0.05$).

The drug release behavior was further assessed by MLRA approach in a one-point method using the percentage of drug release for 3 min (Q_{3min}) and multiple point methods as described as the drug release profiles during 7 min (DE_{7min}). All factors significantly affected the Q_{3min} ($P < 0.05$). Depending on the main effect contribution, the ethanol (-7.96) had higher effect than S-SNEDDS loading (6.66). Although, the S-SNEDDS loading had a positive effect on increasing the drug release and ethanol reduced the drug release. Nevertheless, the interaction between them (-7.82) reduced the drug release. Fig. 6a depicts the contour plot of Q_{3min} parameter. The highest Q_{3min} value was obtained at the highest level of S-SNEDDS loading without ethanol. Meanwhile, the lowest Q_{3min} value was observed in the highest level of S-SNEDDS loading with a 1 part of ethanol as the diluent. A similar result was observed in the DE_{7min} value that the SNEDDS loading affected the increasing the drug released, but the ethanol did not significantly affect the DE_{7min} ($P > 0.05$). However, the pattern of the direction of the main effect and interaction coefficient was similar to the Q_{3min} parameter. The contour plot of DE_{7min} (Fig. 6b) proved the significant effect of S-SNEDDS loading and their interaction. Superimposed contour plot (data not shown), a combination of all contour plots suggested that the ideal combination was achieved at the high level of SNEDDS loading until 20% and solidification without the diluent.

DISCUSSION

According to the particle size (< 300 nm) and zeta potential, SNEDDS characteristics fulfilled the requirements of nanoemulsion characteristics. In addition, these characteristics enhanced the biological transport trough the mucus as per oral barrier absorption (25). In our previous investigation, the solidification using soluble carrier which had absorption mechanism did not alter the particle size and its distribution. The drug load was good enough for incorporation of SNEDDS formulation into mannitol porous carrier for considering the PVT potency (2 and 4 mg per administration) (26). In our perspective, the higher loading of SNEDDS formulation to obtain high potency of the drug in the solid SNEDDS, the more efficient way was (7). However, it reduced physical properties *e.g.* flowability and compactibility (12) and nanodroplet formation owing to interaction with a carrier (27,28). Physical modification of mannitol has been successful for enhancing the surface area and pore characteristics. Therefore, the higher surface area, the greater the probability of SNEDDS formulation contacted to the surface of the carrier (4,12).

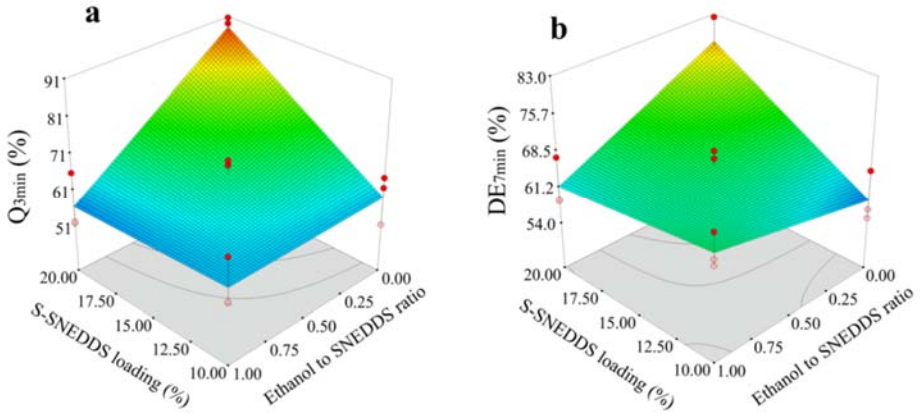

Fig. 6. Contour plot of (a) the drug release at 3 min and (b) dissolution efficiency during 7 min. Q_{3min}, drug release at 3 min; DE_{7min}, dissolution efficiency during 7 min; SNEDDS, self-nano emulsifying drug delivery system.

In order to elucidate the interaction between SNEDDS and carrier, vibrational spectroscopy and thermal analyses were performed. The vibrational spectra suggested that four spectra of solid S-SNEDDS had a similar pattern. Despite no crystallinity packaging in the crystal lattice structure, both SNEDDS composition and PVT dispersed molecularly, and the main reason of the additive effect of the mixture as linear as the concentration *i.e.* mannitol porous material had higher concentration (80-90%) than PVT 0.5-1.0% and S-SNEDDS (9.5-19%), the mannitol vibration peak was the most dominant. Therefore, the specific vibration peaks of PVT were not observed adequately. These ATR-FTIR spectra revealed that there was no vibrational interaction observed in the incorporation of S-SNEDDS to the mannitol porous carrier. Further characterization as a confirmation of interaction was performed.

The thermogram suggested that ethanol in the solidification process affected the thermal behavior. It formed an azeotropic mixture with SNEDDS formulation in which it could not be eliminated during solidification. Further investigation might be performed by determination of ethanol content in this system. Finally, ethanol and SNEDDS loading did not alter the thermal behavior qualitatively. Therefor there was no significant interaction. Although, it could be detected quantitatively by alteration the enthalpy. Therefore, the ethanol as the diluent did not significantly alter the surface characteristics. Although, the partial disturbance and breaking of the spherical carrier in the high SNEDDS loading was observed particularly in the formulation without diluent. Thus, it was indicated the saturated condition of PVT on the liquid SNEDDS could be incorporated into the carrier completely without crystallization and crystal growth.

Design of experiment as a simultaneous approach to assess the effect of SNEDDS loading and ethanol on the solidification of PVT SNEDDS formulation has been successfully implemented (17,24). The additional point in the center of the design enhanced the predictive power of the model and it measured the considering of requirement of additional level of each factor owing to the model function *i.e.* quadratic and cubic models (17,18). The more appropriate model fitting, the more adequate of the model was, thus it was purposed to avoid missleading on the model prediction (24). All models could be used to predict and assess the response adequately.

The challenge of the incorporation of liquid phase introduced into a solid carrier is the alteration of the solid carrier texture, in which it enhances the wetness of the carrier. Furthermore, it reduces the flowability (4,12). The angle of repose is one of the flowability parameters, it measures the material packaging during flow related to the cohesiveness, interparticle friction, and resistance to movement between particles (29,30). According to the USP, angle of repose is an adequate technique to measure the flowability. The angle of repose of all formulations ranged from 36.0 to 40.5° and it was categorized as fair and aid not needed (29). The ethanol increased the angle of repose in which it reduced the flowability. This result confirmed that the ethanol as a co-solvent formed an azeotropic mixture with the organic component in the S-SNEDDS formulation, thus enhanced the wetness of the solid S-SNEDDS. The greater wetness characteristics, the more cohesive of material was, thus it enhanced the angle of repose (30). The physico-mechanical properties determined the characteristic of the material for further formulation which compaction was needed *e.g.* tablet formulation (31). The incorporation of SNEDDS and ethanol in the carrier reduced the compactibility owing to an increase in the cohesiveness and wetness and the liquid phase coated the particle thus reducing the interparticle bonding during compaction (32). This parameter was not a fundamental aspect if the tablet formulation did not apply as a further formulation.

The rate-limiting step of drug release of solid S-SNEDDS depended on the initial time which affected by water penetration and followed by carrier disintegration and solubilization (6,28). Furthermore, the emulsification occurred spontaneously

after the solubilization of carrier. Particularly, the drug released into the medium under nanodroplet formation by which the drug was loaded in the ultra-fine size of an oily droplet (16,33). The released PVT was limited by the solubility of PVT, meanwhile the capsule shell comprising of a little amount of surfactant promotes the enhancement of PVT solubilization. The ethanol reduced the drug release at the initial time owing to reducing the emulsification process and enhancing the interaction between absorbed S-SNEDDS and carrier as a water-bound system. On contrary, the addition of ethanol in the SNEDDS without incorporation into a carrier enhanced the isotropic condition of microemulsion (34). This result suggested that ethanol promoted a reduction of drug release by enhancement of interaction between mannitol as a carrier and hydrophilic groups in the SNEDDS components. A blatant interaction was observed in the middle of the design to increase the S-SNEDDS loading and decrease the ethanol.

CONCLUSION

The effects of S-SNEDDS loading and ethanol on the solidification were fully understood. The S-SNEDDS loading had no significant effect on the flowability properties. In addition, the ethanol promoted to a negative effect owing to the increasing the wetness of the solid S-SNEDDS. The reduction of the compactibility profile was observed owing to increasing the S-SNEDDS concentration and the diluent effect. Moreover, the drug release profile was not affected by the ethanol. Finally, the design model suggested that the solidification without ethanol as a diluent was preferable and had no significant effect on the flow, compaction, and drug release behaviors.

ACKNOWLEDGEMENTS

This research was financially supported by "*Beasiswa Unggulan Dosen Indonesia (BUDI)*", Indonesian Endowment Fund for Education (LPDP). The authors would like to thank Gattefose (Saint-Priest, France) for providing the excipients. Syaiful Choiri and Ilham Kuncahyo would like to thank Indonesian Endowment Fund for Education (LPDP) for funding their scholarship.

REFERENCES

1. Mokarizadeh M, Kafil HS, Ghanbarzadeh S, Alizadeh A, Hamishehkar H. Improvement of citral antimicrobial activity by incorporation into nanostructured lipid carriers: a potential application in food stuffs as a natural preservative. Res Pharm Sci. 2017;12(5):409-415.
2. Ghasemiyeh P, Mohammadi-Samani S. Solid lipid nanoparticles and nanostructured lipid carriers as novel drug delivery systems: applications, advantages and disadvantages. Res Pharm Sci. 2018;13(4):288-303.
3. Bandyopadhyay S, Katare OP, Singh B. Development of optimized supersaturable self-nanoemulsifying systems of ezetimibe: effect of polymers and efflux transporters. Expert Opin Drug Deliv. 2014;11(4):479-492.
4. Chavan RB, Modi SR, Bansal AK. Role of solid carriers in pharmaceutical performance of solid supersaturable SEDDS of celecoxib. Int J Pharm. 2015;495(1):374-384.
5. Pouton CW. Formulation of poorly water-soluble drugs for oral administration: Physicochemical and physiological issues and the lipid formulation classification system. Eur J Pharm Sci. 2006;29 (3-4):278-287.
6. Christophersen PC, Christiansen ML, Holm R, Kristensen J, Jacobsen J, Abrahamsson B, *et al*. Fed and fasted state gastro-intestinal in vitro lipolysis: *In vitro in vivo* relations of a conventional tablet, a SNEDDS and a solidified SNEDDS. Eur J Pharm Sci. 2014;57:232-239.
7. Inugala S, Eedara BB, Sunkavalli S, Dhurke R, Kandadi P, Jukanti R, *et al*. Solid self-nanoemulsifying drug delivery system (S-SNEDDS) of darunavir for improved dissolution and oral bioavailability: In vitro and in vivo evaluation. Eur J Pharm Sci. 2015;74:1-10.
8. Hassan TH, Metz H, Mäder K. Novel semisolid SNEDDS based on PEG-30-dipolyhydroxystearate: development and characterization. Int J Pharm. 2014;477(1-2):506-518.
9. Mustapha O, Kim KS, Shafique S, Kim DS, Jin SG, Seo YG, *et al*. Development of novel cilostazol–loaded solid SNEDDS using a SPG membrane emulsification technique: Physicochemical characterization and *in vivo* evaluation. Colloids Surf B Biointerfaces. 2017;150:216-222.
10. Mandić J, Zvonar Pobirk A, Vrečer F, Gašperlin M. Overview of solidification techniques for self-emulsifying drug delivery systems from industrial perspective. Int J Pharm. 2017;533(2): 335-345.

11. Cirri M, Roghi A, Valleri M, Mura P. Development and characterization of fast-dissolving tablet formulations of glyburide based on solid self-microemulsifying systems. Eur J Pharm Biopharm. 2016;104:19-29.
12. Oh DH, Kang JH, Kim DW, Lee BJ, Kim JO, Yong CS, *et al*. Comparison of solid self-microemulsifying drug delivery system (solid SMEDDS) prepared with hydrophilic and hydrophobic solid carrier. Int J Pharm. 2011;420(2):412-418.
13. Rahman MA, Mujahid M, Rahman MA, Mujahid M. Development of self-nanoemulsifying tablet (SNET) for bioavailability enhancement of sertraline. Braz J Pharm Sci. 2018;54(1):e17232.
14. Peng T, Zhang X, Huang Y, Zhao Z, Liao Q, Xu J, *et al*. Nanoporous mannitol carrier prepared by non-organic solvent spray drying technique to enhance the aerosolization performance for dry powder inhalation. Sci Rep. 2017;7:46517-46527.
15. Pomázi A, Ambrus R, Sipos P, Szabó-Révész P. Analysis of co-spray-dried meloxicam-mannitol systems containing crystalline microcomposites. J Pharm Biomed Anal. 2011;56(2):183-190.
16. Agrawal AG, Kumar A, Gide PS. Formulation of solid self-nanoemulsifying drug delivery systems using N-methyl pyrrolidone as cosolvent. Drug Dev Ind Pharm. 2015;41(4):594-604.
17. Ainurofiq A, Choiri S, Azhari MA, Siagian CR, Suryadi BB, Prihapsara F, *et al*. Improvement of meloxicam solubility using a β-cyclodextrin complex prepared via the kneading method and incorporated into an orally disintegrating tablet. Adv Pharm Bull. 2016;6(3):399-406.
18. Choiri S, Ainurofiq A, Ratri R, Zulmi MU. Analytical method development of nifedipine and its degradants binary mixture using high performance liquid chromatography through a quality by design approach. IOP Conf Ser Mater Sci Eng. 2018;333(1):12064-12070.
19. Dash RN, Mohammed H, Humaira T, Ramesh D. Design, optimization and evaluation of glipizide solid self-nanoemulsifying drug delivery for enhanced solubility and dissolution. Saudi Pharm J. 2015;23(5):528-540.
20. Long AG, Williams RL. The United States Pharmacopoeia 41 - National Formulary 36. Rockville, USA: The United States Pharmacopeial Convention; 2018. pp. 7481-7485.
21. Gong X, Chang SY, Osei-Yeboah F, Paul S, Perumalla SR, Shi L, *et al*. Dependence of tablet brittleness on tensile strength and porosity. Int J Pharm. 2015;493(1-2):208-213.
22. Zhao Y, Wang C, Chow AH, Ren K, Gong T, Zhang Z, *et al*. Self-nanoemulsifying drug delivery system (SNEDDS) for oral delivery of Zedoary essential oil: formulation and bioavailability studies. Int J Pharm. 2010;383(1-2):170-177.
23. Khan KA. The concept of dissolution efficiency. J Pharm Pharmacol. 1975;27(1):48-49.
24. Ainurofiq A, Choiri S. Development and optimization of a meloxicam/β-cyclodextrin complex for orally disintegrating tablet using statistical analysis. Pharm Dev Technol. 2018;23(5):464-475.
25. Griesser J, Hetényi G, Kadas H, Demarne F, Jannin V, Bernkop-Schnürch A. Self-emulsifying peptide drug delivery systems: How to make them highly mucus permeating. Int J Pharm. 2018;538(1-2): 159-166.
26. Masana L. Pitavastatin: Potential in Clinical PracticePitavastatin – from clinical trials to clinical practice. Atheroscler Suppl. 2010;11(3):15–22.
27. Kim KS, Yang ES, Kim DS, Kim DW, Yoo HH, Yong CS, *et al*. A novel solid self-nanoemulsifying drug delivery system (S-SNEDDS) for improved stability and oral bioavailability of an oily drug, 1-palmitoyl-2-linoleoyl-3-acetyl-rac-glycerol. Drug Deliv. 2017;24(1):1018-1025.
28. Seo YG, Kim DW, Yousaf AM, Park JH, Chang PS, Baek HH, *et al*. Solid self-nanoemulsifying drug delivery system (SNEDDS) for enhanced oral bioavailability of poorly water-soluble tacrolimus: physicochemical characterisation and pharmacokinetics. J Microencapsul. 2015;32(5): 503-510.
29. Kuncahyo I, Choiri S. The influence of magnesium stearate, purified talc and combination of both on ternary/quaternary interactive mixture of freely and poorly water-soluble drug. Int J Pharm Pharm Sci. 2014;7(1):397-402.
30. Mangal S, Gengenbach T, Millington-Smith D, Armstrong B, Morton DAV, Larson I. Relationship between the cohesion of guest particles on the flow behaviour of interactive mixtures. Eur J Pharm Biopharm. 2016;102:168-177.
31. Tarlier N, Soulairol I, Bataille B, Baylac G, Ravel P, Nofrerias I, *et al*. Compaction behavior and deformation mechanism of directly compressible textured mannitol in a rotary tablet press simulator. Int J Pharm. 2015;495(1):410-419.
32. Castrati L, Mazel V, Busignies V, Diarra H, Rossi A, Colombo P, *et al*. Comparison of breaking tests for the characterization of the interfacial strength of bilayer tablets. Int J Pharm. 2016;513 (1-2):709-716.
33. Shanmugam S, Baskaran R, Balakrishnan P, Thapa P, Yong CS, Yoo BK. Solid self-nanoemulsifying drug delivery system (S-SNEDDS) containing phosphatidylcholine for enhanced bioavailability of highly lipophilic bioactive carotenoid lutein. Eur J Pharm Biopharm. 2011;79(2):250-257.
34. Szumała P. Structure of microemulsion formulated with monoacylglycerols in the presence of polyols and ethanol. J Surfactants Deterg. 2015;18:97-106.